

National conference on Nanomaterials for Environmental [NCNER-2015]
19th & 20th of March 2015

Dielectric studies on Bismuth substituted Zinc aluminate Nanoparticles

Vengat Savunthari Kiran and Shanmugam Sumathi*

Materials chemistry division, SAS, VIT University, Vellore-632014, India

Abstract: Zinc aluminate ($ZnAl_2O_4$) and bismuth substituted zinc aluminate ($ZnAl_{1.9}Bi_{0.1}O_4$) compounds of nano size were synthesized by co-precipitation method using ammonia as the precipitating agent. The synthesized compounds were characterized by Powder X-ray diffraction (XRD), Fourier Transform Infrared spectroscopy (FTIR), Scanning Electron microscopy (SEM). The average crystallite size of the sample varied from 5.5 to 5.1 nm. Influence of bismuth substitution on the dielectric constant and dielectric loss of zinc aluminate was studied at room temperature as a function of frequency (10 Hz – 5 KHz). These studies suggest that dielectric dispersion was due to Maxwell-Wagner Interfacial Polarization. Variation in dielectric constant and dielectric loss was noticed with the substitution of bismuth in zinc aluminate.

Keywords: Zinc aluminate, spinel oxide, Dielectric property, nanomaterial, X-ray diffraction.

Introduction

Spinel oxides have the general formula of AB_2O_4 . Where A is divalent and B is trivalent metal ion. A^{2+} ions occupy tetrahedral voids, B^{3+} ions occupy octahedral voids and the anions are arranged in cubic closed packed array^{1,2}. Among the aluminates, zinc aluminates ($ZnAl_2O_4$) nanoparticles has received the attention in various fields because of its interesting properties such as low surface acidity, high thermal stability, high mechanical strength, better diffusion, low temperature sintering ability and chemical resistance^{3,4,5,6,7}. In general zinc aluminate is used in sensors, high temperature ceramic materials, electronics, catalysis and catalyst support^{8,9,10}. Current research in nanotechnology is reducing the size of the particle to the nano level, in order to compare the properties of the bulk material and nanomaterial and also to study the effect of substituent on the properties such as optical, electronic, catalysis at the nanolevel^{11,12}.

Kurien et al¹³ reported the dielectric properties of aluminates in terms of particle size, temperature and frequency. It is observed from the literature that the dielectric property of the spinel oxide can be altered by doping of the divalent or trivalent ions at the aluminium site in spinel aluminates. Since, the polarization in spinel aluminates is determined mainly by the trivalent aluminium ion at the octahedral site^{14,15,16,17}. Mostly zinc aluminate compounds are studied for catalysis, luminescent properties. But limited reports are available on the dielectric property. Abdul Jammal reported on the dielectric property of zinc aluminate¹⁸. Calcium doped zinc aluminates are reported for microwave dielectric properties¹⁹. Tabaza et al reported the effect of bismuth doping on the luminescent properties of magnesium aluminate²⁰. Kim et al reported on the phosphorescence

behaviour of bismuth doped zinc gallate²¹. Bismuth doped zinc aluminate are not explored much like other spinel aluminates. Rare earth substituted spinel aluminates are studied for dielectric properties^{22, 23}. To the best of our knowledge less work is reported on the dielectric property of the doped zinc aluminates.

Zinc aluminate nanoparticles have been synthesised by diverse methods such as sol-gel²⁴, co-precipitation²⁵, hot injection thermolysis²⁶, thermal decomposition²⁷, combustion²⁸ and micro-emulsion²⁹. Among these methods, the co-precipitation method has the advantages such as homogeneity, high specific surface area, high porosity and purity, low temperature preparation and simple process³⁰.

In this present work, Zinc aluminate ($ZnAl_2O_4$) and bismuth substituted zinc aluminate ($ZnAl_{1.9}Bi_{0.1}O_4$) nano crystalline powder are synthesized by co-precipitation method and characterized by various techniques. The dielectric properties of the synthesized compounds are studied at room temperature as function of frequency (10 Hz – 5 KHz).

Experimental

Materials

$Zn(NO_3)_2 \cdot 6H_2O$ (s.d fine 99.0%), $Al(NO_3)_3 \cdot 9H_2O$ (s.d fine 98.0%), $Bi(NO_3)_3 \cdot 5H_2O$ (s.d fine 98.5%) and ammonia solution (s.d fine AR).

Method

Zinc aluminate ($ZnAl_2O_4$) and bismuth substituted zinc aluminate ($ZnAl_{1.9}Bi_{0.1}O_4$) nanoparticles were prepared by co-precipitation method³¹. The details of the procedure is as follows: stoichiometric quantities of $Zn(NO_3)_2 \cdot 6H_2O$, $Al(NO_3)_3 \cdot 9H_2O$ and $Bi(NO_3)_3 \cdot 5H_2O$ were weighed and dissolved in double distilled water. Aqueous ammonia solution was added to the mixture of the solution to maintain the pH value 10.5. The precipitated slurry was filtered and washed several times with distilled water and dried at 80°C for 24 h. The obtained powder was treated at different temperature 300 – 700°C for 4 h with intermittent grinding.

Characterization

The compound was characterized by X-ray diffraction (model D8 advance BRUKER Germany) in the 2theta range 10°-70°. Fourier transforms infrared spectrophotometer was recorded in the range 2500-400 cm^{-1} using FT-IR SHIMADZU model and surface morphology was analysed by scanning electron microscopy (ZESIS EVO18). Sintered disc shaped samples with silver electrodes were subjected to the measurements of dielectric constant and dielectric loss using an HP4194 analyzer.

Results and discussion

Powder X-ray diffraction (XRD)

The powder XRD pattern of zinc aluminate and bismuth substituted zinc aluminate ($ZnAl_{2-x}Bi_xO_4$ x=0 and 0.1) are shown in Figure1. All the diffraction peaks can be fully indexed based on 2theta peaks at 19.42°, 31.40°, 37.13°, 46.52°, 55.80°, 59.93° and 66.08° which are corresponding to (111), (220), (311), (400), (422), (511) and (440) diffraction lines showing that zinc aluminate is a cubic crystal system spinel structure (JCPDS file no.96-101-1002) of $Fd3m$ space group. The lattice parameter (a) is calculated from the most intense peak (311) using the formula³².

$$a = d [(h^2+k^2+l^2)]^{1/2}$$

Where h, k and l are miller indices, d is inter planar distance and 'a' is lattice parameter. Increase in lattice parameter is observed because of the substitution of bismuth in zinc aluminate (Table 1). This could be due to large ionic radii of bismuth (1.03 Å) than aluminium ion (0.53 Å). Average crystalline size of the nanoparticle is calculated using Debye – Scherer formula¹⁸.

$$D = \frac{0.9\lambda}{\beta \cos \theta}$$

Where, D is average crystalline size, λ is X-ray wavelength, β is full-width at half maximum (FWHM) and θ is Bragg's angle was calculated intense peak (311). Average crystallite size is decreased from 5.590 nm to

5.145 nm by bismuth substitution (Table 1).

Table 1: Lattice parameter and average crystallite size of the synthesized compounds

Compound	Lattice parameter(\AA)	Crystallite size (nm)	Volume (\AA^3)
ZnAl_2O_4	8.023	5.590	516.43
$\text{ZnAl}_{1.9}\text{Bi}_{0.1}\text{O}_4$	8.083	5.145	528.10

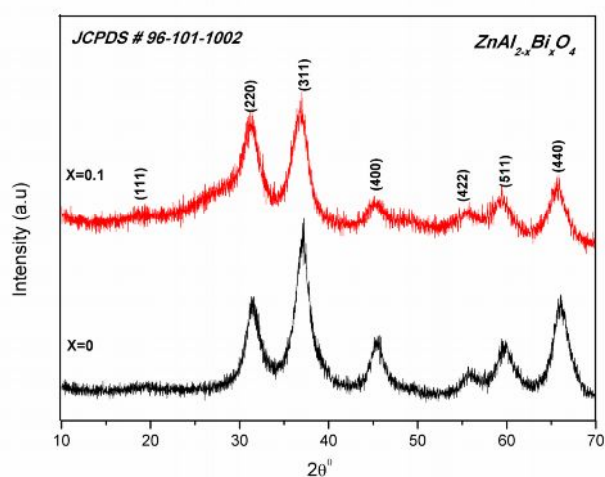


Figure 1. Powder XRD pattern of ZnAl_2O_4 and $\text{ZnAl}_{1.9}\text{Bi}_{0.1}\text{O}_4$

Fourier Transform infrared spectroscopy (FT-IR)

Figure 2 shows the FT-IR spectrum of parent and bismuth substituted zinc aluminates nanoparticles. The three bands which are observed in the range $400\text{--}700\text{cm}^{-1}$ are characteristics of zinc aluminate spinel structure. The bands at 657 and 549 cm^{-1} are due to symmetric stretching and bending modes of AlO_6 and the band at 484 cm^{-1} is due to asymmetric stretching mode of AlO_6 group³³.

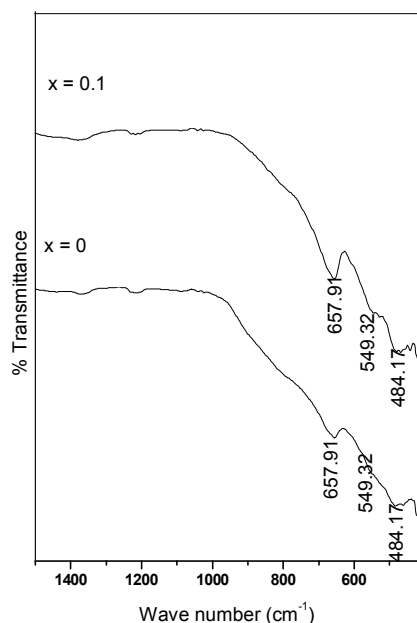


Figure 2. FT-IR spectra of ZnAl_2O_4 and $\text{ZnAl}_{1.9}\text{Bi}_{0.1}\text{O}_4$

Scanning electron microscopy (SEM)

Scanning electron microscopic images are given in Figure 3. Micro structural image of zinc aluminate shows some distinguished grains of different shapes with some agglomeration. But in the case of substituted zinc aluminates more agglomerated cluster like morphology is observed.

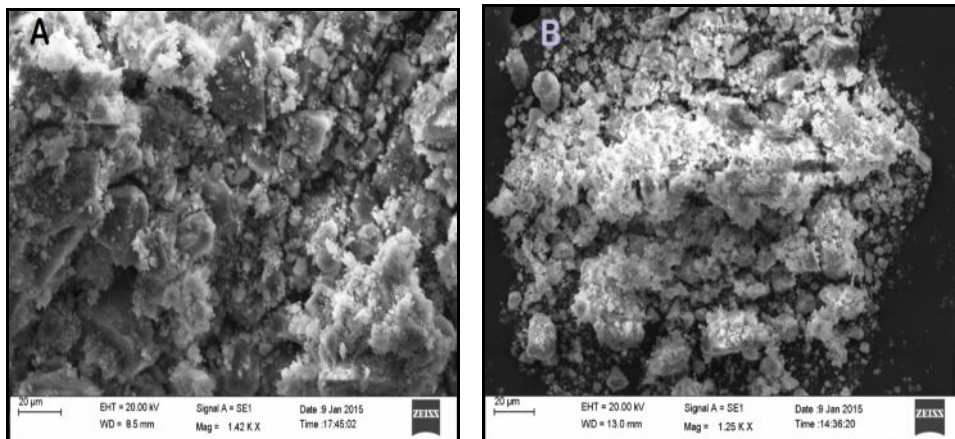


Figure 3. SEM images of $ZnAl_2O_4$ and $ZnAl_{1.9}Bi_{0.1}O_4$

Dielectric properties

The variation of dielectric constant (ϵ') and dielectric loss ($\tan\delta$) with applied frequency (10 Hz – 5 KHz) for zinc aluminate and bismuth substituted zinc aluminate at room temperature are given in Figure 4 and Figure 5. It can be seen that the dielectric constant decreases with increase in frequencies in both the unsubstituted and bismuth substituted compounds. According to Maxwell-Wagner model³⁴ and Koops theory³⁵, dielectric medium consists of poorly conductive grain boundaries and conductive grains. In the presence of the external electric field, charge carriers can easily move through the grains but accumulate in the grain boundaries. This causes large polarization and enhanced dielectric constant at lower frequencies. Increase in the surface area of the grains in the nano regime could be one of the reasons for enhanced dielectric constant because of large surface polarization³⁶. The substitution of bismuth increases the dielectric constant of zinc aluminate. Rajeevan *et al* also reported the same behaviour for bismuth substituted cobalt manganite³⁷. The decrease in average crystallite size by the introduction of bismuth could be one of the reasons for enhanced dielectric constant. Since, the number of grain per unit volume increases with decrease in average crystallite size³⁸.

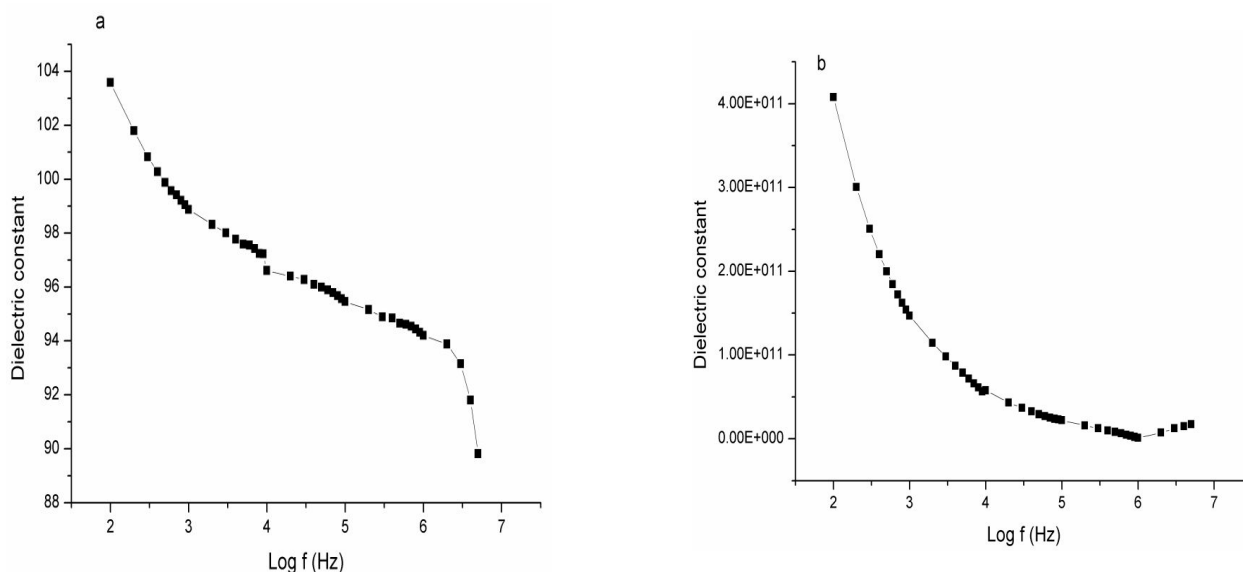


Figure 4. Variation of dielectric constant (ϵ') a) zinc aluminate b) bismuth substituted zinc aluminates at room temperature

From the Figure 5 it is observed that dielectric loss decreases continuously with the frequencies, this may be due to space charge polarization³⁶. A slight increase in dielectric loss is noted at lower frequency in the bismuth substituted compound than the parent compound. But at higher frequency the dielectric loss of both compounds are almost constant. Saha et al reported that this very low dielectric loss in the high frequency region makes this material suitable for high frequency applications³⁶.

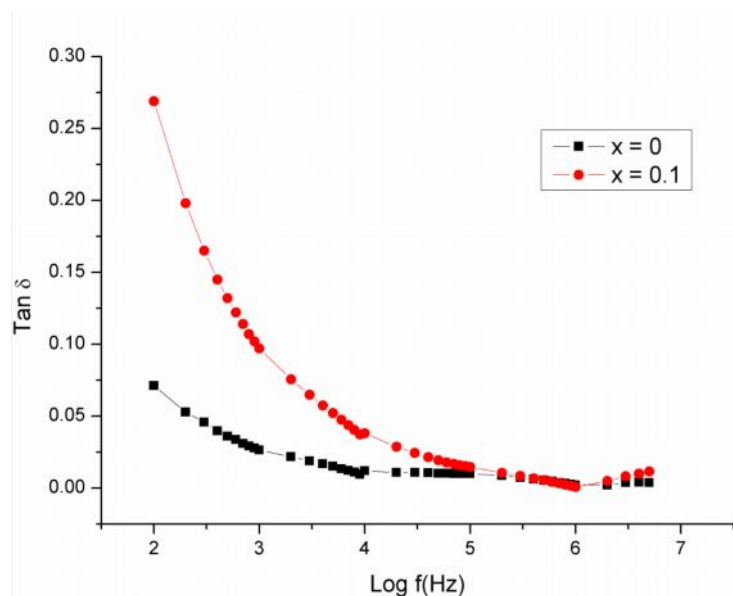


Figure 5. Variation of dielectric loss ($\tan \delta$) of zinc aluminate and bismuth substituted zinc aluminates at room temperature

Conclusion

Bismuth substituted zinc aluminates ($\text{ZnAl}_{2-x}\text{Bi}_x\text{O}_4$ $x=0, 0.1$) spinel type sample have been prepared by co-precipitation method using ammonia as the precipitating agent. XRD patterns revealed the formation of pure phase without any impurities. The substitution of bismuth increases the lattice parameter and decreases the particle size. An increase in the dielectric constant (ϵ') and dielectric loss tangent ($\tan \delta$) of zinc aluminates at room temperature have been observed due to the substitution of bismuth ion. The low dielectric constant and dielectric loss at high frequency region make this material suitable for high frequency applications.

Acknowledgements

The authors thank the VIT University management for providing all required facilities to carry out the experiments. We also thank Dr. Rajanbabu and Mr. Gowrisankar for the dielectric studies.

References:

1. Sharma RK, Ghose R. Synthesis and characterization of nanocrystalline zinc aluminate spinel powder sol-gel method. *Ceram. Int.*, 2014, 40; 3209-3214.
2. Anchieta CG, Daniela Sallet, Edson L, Foletto, Syllos S, da Silva, Chiavone-Filho O, ClaudiAO, Nascimento D. Synthesis of ternary zinc spinel oxides and their application in the photo degradation of organic pollutant. *Ceram. Int.*, 2014, 40; 4173-4178.
3. Wei X, Chen D. Synthesis and characterization of nanosized zinc aluminate spinel by sol-gel technique. *Mater. Lett.*, 2006, 60; 823-827.
4. Zawadzki M, Staszak W, Suarez FEL, Gomez MJI, Lopez AB. Preparation, characterization and catalytic performance for soot oxidation of copper-containing ZnAl_2O_4 spinels. *Appl. Catal., A.*, 2009, 371; 92-98.
5. Duan X, Yuan D, Wang X, Xu H. Synthesis and characterization of nanocrystalline zinc aluminum spinel by a new sol-gel method. *J. Sol-Gel Sci. Technol.*, 2005, 35; 221-224.

6. Ge DL, Fan YJ, Qi CL, Sun ZX. Facile synthesis of highly thermostable mesoporous ZnAl_2O_4 with adjustable pore size. *J. Mater. Chem.*, 2013, 1; 1651–1658.
7. Alves CT, Oliveira A, Carneiro SAV, Silva AG, Andrade HMC, Vieira de Melo SAB, Torres EA. Transesterification of waste frying oil using a zinc aluminate catalyst. *Fuel Process. Technol.*, 2013, 106; 102–107.
8. Fan G, Wang J, Li F. Synthesis of high-surface-area micro mesoporous ZnAl_2O_4 catalyst support and application in selective hydrogenation of ochloronitrobenzene. *Catal. Commun.*, 2011, 15; 113–117.
9. Farhadi S, Panahandehjoo S. Spinel-type zinc aluminate (ZnAl_2O_4) nanoparticles prepared by the co-precipitation method: a novel, green and recyclable heterogeneous catalyst for the acetylation of amines, alcohols and phenols under solvent-free conditions. *Appl. Catal., A.*, 2010, 382; 293–302.
10. Ranjbar M, Niasari MS, Mashkani SMH. Microwave synthesis and characterization of spinel-type zinc aluminate nanoparticles. *J. Inorg. Organomet. Polym. Mater.*, 2012, 22; 1093–1100.
11. Siegel RW, What do we really know about the atomic-scale structures of nano phase materials. *J. Phys. Chem. Solids.*, 1994, 55; 1097-1106.
12. Sugimoto M. The Past, Present, and Future of Ferrites. *J. Am. Chem. Soc.*, 1999, 82; 269-280.
13. Kurien S, Mathew J, Sebastain S, Potty SN, George KC. Dielectric behavior and ac electrical conductivity of nanocrystalline nickel aluminate. *Mater. Chem. Phys.*, 2006, 98; 470–476.
14. Iqbal MJ, Farooq S. Effect of doping of divalent and trivalent metal ions on the structural and electrical properties of magnesium aluminate. *Mater. Sci. Eng., B.*, 2007, 136; 140-147.
15. Iqbal MJ, Ismail B. Electric, dielectric and magnetic characteristics of Cr^{3+} , Mn^{3+} and Fe^{3+} substituted MgAl_2O_4 : Effect of pH and annealing temperature. *J. Alloys Compd.*, 2009, 472; 434-440.
16. Iqbal MJ, Kishwar B. Electrical properties of $\text{MgAl}_{2-2x}\text{Zr}_x\text{M}_x\text{O}_4$ ($\text{M} = \text{Co}, \text{Ni}$ and $x = 0.00\text{--}0.20$) synthesized by co precipitation technique using urea. *Mater. Res. Bull.*, 2008, 44; 753-758.
17. Iqbal MJ, Ismail B. Correlation between structural and electrical properties of $\text{Mg}_{1-2x}\text{Zn}_x\text{Ni}_x\text{Al}_2\text{O}_4$ ($x = 0.0\text{--}0.5$) ceramic nanomaterials synthesized by a urea assisted microwave combustion method. *J. Alloys Compd.*, 2010, 504; 440-445.
18. Muhammad Abdul Jamal E, Sakthi Kumar D, Anantharaman MR. On structural, optical and dielectric properties of zinc aluminate nanoparticles. *Bull. Mater. Sci.*, 2011, 34; 251-259.
19. Wan Jalal WN, Abdullah H, Zulfakar MS. Effect of Zn Site for Ca Substitution on Optical and Microwave Dielectric Properties of ZnAl_2O_4 Thin Films by Sol Gel Method. *Adv. Mater. Sci. Eng.*, 2014, Article ID 619024, 8 pages.
20. Tabaza WAI, Swart HC, Kroon RE. Optical properties of Bi and energy transfer from Bi to Tb in MgAl_2O_4 phosphor. *J. Lumin.*, 2014, 148; 192–197.
21. Kima WN, Parka HL, Kimb GC. Lithium solubility limit in $\text{ZnGa}_2\text{O}_4:\text{Bi}_{0.001}^{3+}, \text{Li}^+$ phosphor. *Mater. Lett.*, 2005, 59; 2433 – 2436.
22. Samkaria R, Sharma V. Structural, dielectric and electrical studies of $\text{MgAl}_{2-2x}\text{Y}_{2x}\text{O}_4$ ($x=0.00\text{--}0.05$) cubic spinel nano aluminate. *J. Electroceram.*, 2013, 31; 67–74.
23. Samkaria R, Sharma V. Effect of rare earth yttrium substitution on the structural, dielectric and electrical properties of nanosized nickel aluminate. *Mater. Sci. Eng., B.*, 2013, 178; 1410– 1415.
24. Sanpo N, Christopher C, Berndt, Wen C, Wang J. Transition metal-substituted cobalt ferrite nanoparticles for biomedical applications. *Acta Biomater.*, 2013, 9; 5830-5837.
25. Nikumbh AK, Pawar RA, Nighot DV, Gugale GS, Sangale MD, Khanvilkar MB, Nagawade AV. Structural, electrical, magnetic and dielectric properties of rare-earth substituted cobalt ferrites nanoparticles synthesized by the co-precipitation method. *J. Magn. Magn. Mater.*, 2014, 355; 201–209.
26. Abdulwahab KO, Malik MA, Paul O'Brien Grigore Timco A. A direct synthesis of water soluble monodisperse cobalt and manganese ferrite nanoparticles from iron based pivalate clusters by the hot injection thermolysis method. *Mater. Sci. Semicond. Process.*, 2014, 27; 303–308.
27. Herrera AP, Polo-Corrales L, Chavez E, Cabarcas-Bolivar J, Oswald NC, Uwakweh, Rinaldi R. Influence of aging time of oleate precursor on the magnetic relaxation of cobalt ferrite nanoparticles synthesis by the thermal decomposition method. *J. Magn. Magn. Mater.*, 2013, 328; 41-52.
28. Kooti M, Saiahi S, Motamedi H. Fabrication of silver-coated cobalt ferrite nanocomposite and the study of its antibacterial activity. *J. Magn. Magn. Mater.*, 2013, 333; 138-143.
29. Khan MA, Sabir M, Asghar M, Mahmood K, Khan MA, Ahmad I, Sher M, Warsi MF. High frequency dielectric response and magnetic studies of $\text{Zn}_{1-x}\text{Tb}_x\text{Fe}_2\text{O}_4$ nanocrystalline ferrite synthesis by via micro-emulsion technique. *J. Magn. Magn. Mater.*, 2014, 360; 188-192.
30. Sharma RK, Ghose R. synthesis of nanocrystalline CuO-ZnO mixed metal oxide powder by a homogeneous precipitation method. *Ceram. Int.*, 2014, 40; 10919-10926.

31. Ragul G, Sumathi S. Synthesis, Characterization and Photocatalytic Study of Zinc Aluminate Nano powders against Rhodamine-B and Crystal Violet Dyes. *Int. J. Appl. Eng. Res.*, 2013, 8; 19, 2175-2178.
32. Cullity BD, Stock SR. *Elements of X-Ray Diffraction*, third edition, Prentice Hall. 2001, New York.
33. Preudhomme J, Tarte P. Infrared studied of spinel-III: the normal II-III spinel. *Spectrochim. Acta A Mol. Biomol. Spectrosc.*, 1971, 27; 1817-1835.
34. Wagner KW. Zur Theorie der Unvollkommenen Dielektrika. *Annalen der Physik*, Vol. 40, 1913, pp. 817-855.
35. Koops CG. On the Dispersion of Resistivity and Dielectric Constant of Some Semiconductors at Audio frequencies. *Physical Review.*, 1951, 83; 121-124.
36. Saha S, Das B, Mazumder N, Bharati A, Chattopadhyay KK. Effect of Cr doping on the ac electrical properties of MgAl₂O₄ nanoparticles. *J. Sol-Gel Sci. Technol.*, 2012, 61; 518-526.
37. Rajeevan NE, Ravi Kumar, Shukla DK, Pradyumnan PP, Arora SK, Shvets IV. Structural, electrical and magnetic properties of Bi-substituted Co₂MnO₄. *Mater. Sci. Eng., B.*, 2009, 163; 48-56.
38. Ashokkumar M, Muthukumaran S. Effect of Cr-doping on dielectric, electric and magnetic properties of Zn_{0.96}Cu_{0.04}O nanopowders, *Powder Technol.*, 2014, 268; 80-85.
